Published in final edited form as:
J Endocrinol. 2010 March ; 204(3): 241–253. doi:10.1677/JOE-09-0328.

A Novel Spontaneous Mutation of *Irs1* in Mice Results in Hyperinsulinemia, Reduced Growth, Low Bone Mass and Impaired Adipogenesis

Victoria E. DeMambro, **Masanobu Kawai**, **Thomas L. Clemens**, **Keertik Fulzele**, **Jane A. Maynard**, **Caralina Marín de Evsikova**, **Kenneth R. Johnson**, **Ernesto Canalis**, **Wesley G. Beamer**, **Clifford J. Rosen**, and **Leah Rae Donahue**
The Jackson Laboratory (V.E.D., J.A.M., C.M., K.R.J., W.G.B., L.R.D.), Bar Harbor, Maine 04609, USA; Medical Center Research Institute (M.K., C.R.J.), Scarborough, Maine, 04074, USA; John Hopkins University (T.L.C.), Baltimore, MD 21287 USA; Massachusetts General Hospital, (K.F.), Boston, Massachusetts, 02114 USA; Department of Research, Saint Francis Hospital and Medical Center (E.C.), Hartford, Connecticut 06105, USA.

Abstract

A spontaneous mouse mutant, designated 'small' (*sml*), was recognized by reduced body size suggesting a defect in the IGF-I/GH axis. The mutation was mapped to the Chromosome 1 region containing *Irs1*, a viable candidate gene whose sequence revealed a single nucleotide deletion resulting in a premature stop codon. Despite normal mRNA levels in mutant and control littermate livers, Western blot analysis revealed no detectable protein in mutant liver lysates. When compared to control littermates, $Irs1^{sml}/Irs1^{sml}$ ($Irs1^{sml/sml}$) mice are small, lean, hearing impaired, have 20% less serum IGF-I, are hyperinsulinemic and are mildly insulin resistant. $Irs1^{sml/sml}$ mice have low bone mineral density, reduced trabecular and cortical thicknesses and low bone formation rates, while osteoblast and osteoclast numbers were increased in the females but not different in the males compared to $Irs1^{+/+}$ controls. In vitro, $Irs1^{sml/sml}$ bone marrow stromal cell cultures showed decreased alkaline phosphatase positive colony forming units (pre-osteoblasts; CFU-AP+) and normal numbers of tartrate resistant acid phosphatase positive (TRAP) osteoclasts. $Irs1^{sml/sml}$ stromal cells treated with IGF-I exhibited a 50% decrease in AKT phosphorylation, indicative of defective downstream signaling. Similarities between engineered knockouts and the spontaneous mutation of $Irs1^{sml}$ were identified as well as significant differences with respect to heterozygosity and gender. In sum we have identified a spontaneous mutation in the *Irs1* gene associated with a major skeletal phenotype. Changes in the heterozygous $Irs1^{+/sml}$ mice raise the possibility that similar mutations in humans are associated with short stature or osteoporosis.

Keywords

Irs1; bone; growth; adipocytes; hyperinsulinemia

Address all correspondence and requests for reprints to: Victoria DeMambro, 600 Main Street, Bar Harbor, Maine 04609, USA, Phone: (207) 288-6000, Fax: (207) 288-6073, victoria.demambro@yahoo.com.

Declaration of Interest
The authors declare that there is no conflict of interest that would prejudice the impartiality of this work.

Introduction

Insulin and insulin-like growth factor 1 (IGF-I) are critical regulators of growth and metabolism in virtually all mammals. Insulin deficiency syndromes, such as diabetes mellitus type 1 (Type I DM) and low IGF-I levels from growth hormone (GH) deficiency or resistance, are associated with reduced bone mineral density (BMD) and heightened fracture risk (Garnero, Sornay-Rendu et al. 2000; Janghorbani, Feskanich et al. 2006; Janghorbani, Van Dam et al. 2007; Räkel, Sheehy et al. 2008). GH, and hence IGF-I deficiency in children and adults impairs peak bone acquisition and is associated with an increased prevalence of fractures in adulthood (Vestergaard, Jørgensen et al. 2002; Mukherjee, Murray et al. 2004; Giustina, Mazziotti et al. 2008). Similarly, a spontaneous recessive mutation in growth hormone releasing hormone (GHRH) also results in low areal BMD (aBMD) in mice and humans (Donahue and Beamer 1993; Godfrey, Rahal et al. 1993; Maheshwari, Silverman et al. 1998; Baumann 1999). Studies using genetically engineered mice have reinforced the importance of the IGF-I regulatory system in skeletal development. For example, global *Igf1* gene deletion causes a dramatic skeletal phenotype characterized by impaired bone formation and bone resorption (Liu, Baker et al. 1993; Bikle, Majumdar et al. 2001; He, Rosen et al. 2006; Wang, Nishida et al. 2006). Conditional targeted deletion of the type I IGF receptor (*Igf1r*) in osteoblasts causes a profound reduction in trabecular bone volume, osteoblast function and changes in mineralization lag time (Zhang, Xuan et al. 2002). Furthermore, engineered knockout and transgenic over expression of several IGF binding proteins induce marked changes in bone turnover and bone mass (Silha, Mishra et al. 2003; Zhang, Faugere et al. 2003; Atti, Boskey et al. 2005; Ben Lagha, Seurin et al. 2006; DeMambro, Clemmons et al. 2008). Likewise, hepatic specific deletion of *Igf1* (Yakar, Liu et al. 1999), or global deletion of the acid-labile subunit (*Igfals*) in mice promotes marked thinning of the cortical bone compartment, despite minimal changes in linear growth (Yakar, Rosen et al. 2009). Hence, skeletal and circulating IGF-I are essential for optimal peak bone acquisition.

Insulin and IGF-I initiate a chain of intracellular responses and signaling cascades upon binding to tyrosine kinase receptors (IR and IGF1R). The first substrates phosphorylated after ligand binding are the insulin receptor substrate (IRS) proteins. Once phosphorylated by their cognate receptors, these substrates bind to proteins containing Src homology-2 domains, which in turn activate a variety of signaling pathways, including activation of phosphatidylinositol 3-kinase (PI3K) and mitogen-activated protein kinase (MAPK) (Lienhard 1994; White 2003; Niu and Rosen 2005). These intracellular signaling pathways are essential for bone acquisition, since they impact the recruitment, differentiation, and death of osteoblasts (Cornish, Callon et al. 1996; Niu and Rosen 2005). Deletion of *Irs1* (either the $Irs1^{tm1Tka}$ or the $Irs1^{tm1Jos}$ allele) on a mixed B6/CBA hybrid mouse background results in growth retardation, however both female and male mice are relatively healthy and fertile (Araki, Lipes et al. 1994; Tamemoto, Kadowaki et al. 1994). Adult $Irs1^{tm1Tka}$/$Irs1^{tm1Tka}$ ($Irs1^{tm1Tka/tm1Tka}$) mice have low aBMD, delayed fracture healing, with reductions in osteoblast and osteoclast number and function, resulting in decreased bone turnover. These null mice also exhibit impaired anabolic response to intermittent parathyroid hormone (PTH) administration (Ogata, Chikazu et al. 2000; Hoshi, Ogata et al. 2004; Shimoaka, Kamekura et al. 2004; Yamaguchi, Ogata et al. 2005). Both the $Irs1^{tm1Tka/tm1Tka}$ and the $Irs1^{tm1Jos}$/$Irs1^{tm1Jos}$ ($Irs1^{tm1Jos/tm1Jos}$) mice have high serum insulin levels and are insulin resistant despite a lean phenotype, but circulating IGF-I levels were reported not to differ significantly from controls (Araki, Lipes et al. 1994; Tamemoto, Kadowaki et al. 1994; Shirakami, Toyonaga et al. 2002). Thus, several animal models have confirmed that insulin and IGF-I signaling are critical for skeletal acquisition and maintenance.

There are no reports of a spontaneous mutation in the *Irs1* gene leading to complete loss of function in mice or in humans. However, there are numerous studies in humans demonstrating polymorphisms in the *IRS-1* gene associated with metabolic disease, some of which induce amino acid changes and variable responsiveness to insulin and/or IGF-I signaling (Imai, Fusco et al. 1994; Ura, Araki et al. 1996; Le Fur, Le Stunff et al. 2002). The most common polymorphism, the G972R variant, has been associated with type II diabetes mellitus (Almind, Bjørbaek et al. 1993; Sesti 2000; Tok, Ertunc et al. 2006). In contrast, there are no data examining the relationship between these polymorphisms and BMD or fracture risk.

Recently, in the Mouse Mutant Resource at The Jackson Laboratory, we discovered a small mouse phenotype that arose as a spontaneous autosomal recessive mutation on a congenic C3.SW-$H2^b$/SnJ inbred background. Molecular genetic studies revealed that this mutation, designated small (allele symbol *sml*) was due to a frameshift mutation in the *Irs1* gene. This report details the molecular and phenotypic characterization of this mutant and the cellular changes that occur in response to altered IRS-1 signaling. Findings from this study add to insights gained from previous work using genetic engineering and raise important questions about the inter-relationship between the IGF-1 regulatory system and bone acquisition.

Materials and Methods

Mouse Husbandry

The $Irs1^{sml}$ allele is a spontaneous mutation that occurred on an inbred C3.SW-$H2^b$/SnJ mouse strain. All mice used in this study were produced and maintained in our research colony at the Jackson Laboratory (Bar Harbor, Maine). Mice were housed in groups of 4 or 5 of the same sex within polycarbonate boxes of 324 cm^2 in area, on sterilized shavings of Northern White Pine. Colony environmental conditions included 14:10 hour light:dark cycles, with free access to acidified water (pH 2.5 with HCL to retard bacterial growth) and irradiated NIH-31 diet containing 6% fat, 19% protein, Ca:P 1.15:0.85, plus vitamin and mineral fortified (Purina Mills International, Gray Summit, MO, USA). All studies were conducted using groups of mutant, heterozygous and wildtype male and female mice. All procedures involving mice were reviewed and approved by the Institutional Animal Care and Use Committee of The Jackson Laboratory.

Genetic Mapping

To map the *sml* mutation, 204 F_2 mice were produced from an intercross between (C3.SW-$H2^b$/SnJ-*sml* × CAST/Ei) F_1 hybrid mice. Genomic DNA from F_2 mice was prepared and genotyped using Mit marker primer pairs as described previously (Gagnon, Longo-Guess et al. 2006). The *sml* mutation was mapped utilizing recombination frequencies and the Map Manager Program (Manly, Cudmore et al. 2001).

Sequencing of the Irs1 Gene

PCR primers used to amplify exons 1 and 2 of the mouse *Irs-1* gene for sequence comparisons between mutant and control are given in Table 1. PCR reaction conditions were described previously (Gagnon, Longo-Guess et al. 2006). PCR-amplified products were purified using the Qiaquick PCR Purification Kit (Qiagen Inc., Valencia, CA, USA). DNA was sequenced using an Applied Biosystems 373A DNA Sequencer (Applied Biosystems, Foster City, CA, USA). The same primers used for PCR amplification were also used for sequencing.

Genotyping of the Irs1^{sml} colony

To genotype this mouse colony we recognized that the deletion of the one adenine nucleotide in Exon 1 created a restriction enzyme recognition site, which *Taq1* recognizes (T-CGA). We designed primers (*Irs1F* 5' - CAA GGA GGT CTG GCA GGT TA - 3' and *Irs1R* 5' - CCC ACC TCG ATG AAG AAG AA - 3') to amplify the region of interest and then digested with *Taq1* restriction enzyme per the manufacturer's instructions. The digested products yielded a control band of 190 bp, with a mutant band of 171 bp.

Quantitative Real Time PCR

RNA was extracted from the femurs of four 8 week old *Irs1*$^{sml/sml}$ and *Irs1*$^{+/+}$ control mice as described previously (DeMambro, Clemmons et al. 2008). Briefly, femurs were isolated and snap frozen in liquid nitrogen, RNA was then isolated using the Total RNA isolation system (Promega, Madison, WI, USA) as per the manufacturer's instructions. DNA was then removed from the RNA samples using The DNA-free DNase Treatment & Removal Reagents (Ambion, Inc., Austin, TX, USA). RNA quality and quantity were assessed using an Agilent bioanalyzer (caliper technologies Corp., Hopkinton, MA, USA). Four Hundred nanograms of RNA was then converted to cDNA in a reverse transcription reaction using the MessageSensor RT Kit (Ambion, Inc.) and random decamers as primers. The cDNA was then diluted 1:5 with water. Quantification of mRNA expression was carried out using an iQ SYBR Green Supermix in a iQ5 thermal cycler and detection system (BioRad, Hercules, CA, USA). GAPDH was used as an internal standard control gene for all quantification. Primer sequences used in this study are as follows: *Rankl* (Forward: 5'-TAC TTT CGA GCG CAG ATG GAT-3', Reverse: 5'-CTG CGT TTT CAT GGA GTC TCA-3'), *Osteroprotegerin* (Forward: 5'-TCC GGC GTG GTG CAA G-3', Reverse: 5'-AGA ACC CAT CTG GAC ATT TTT TG-3'), *Gapdh* (Forward: 5'- TGA ACG GGA AGC TCA CTG G-3', Reverse: 5'-TCC ACC ACC CTG TTG CTG TA-3').

Western blotting

Mouse livers were collected, frozen in liquid nitrogen and stored at −80°C until processing. Total cellular protein lysates were prepared in buffer consisting of 50mM Tris base (pH 8.2), 150 mM NaCl, 1% Igepal, and Complete protease inhibitor cocktail tablets (Roche, Chicago, IL, USA) for 30 min at 4°C, followed by centrifuging at 10,000*g* for 20 min at 4°C. For immuno-precipitation cell lysates were incubated with a rabbit anti C-terminus IRS-1 antibody (Upstate #06-248, Millapore, Billerica, MA, USA) for 1h at 4°C. The immunocomplexes were then collected using a Immunoprecipitation Kit Protein A (#1719394 Roche) per the manufacturer's instructions. Proteins were resolved on 10% SDS-polyacrylamide gels and transferred to Polyvinylidene fluoride (PVDF) membranes (Millipore). Membranes were blocked with 5% non-fat dry milk (BioRad), then incubated with the same anti C-terminus IRS-1 antibody followed by a horseradish peroxidase (HRP) conjugated donkey anti-rabbit antibody (Santa Cruz #sc-2317). Signal was detected using an enhanced chemiluminescence kit (Amersham, Piscataway, NJ, USA).

The calvarial cells post treatment were washed twice with ice-cold PBS and resuspended in lysis radioimmunoprecipitation assay buffer (RIPA) buffer supplemented with protease and phosphatase inhibitors (Sigma Aldrich, St. Louis, MO, USA). Cell lysates were homogenized by rotating at 4°C for 30 min and then centrifuged at 14,000 rpm for 20 min at 4°C. Protein concentrations were measured in the supernatant using Bradford's reagent (Bio-Rad). Proteins were resolved on 10% SDS–polyacrylamide gels and transferred to PVDF membranes. Membranes were incubated with antibodies for phosphorylated AKT (cell signaling #9271, Danvers, MA, USA) or total AKT (cell signaling #9272) followed by HRP-conjugated goat anti-rabbit antibody (cell signaling #7074). In a separate set of experiments calvarial cells post treatment were immunoprecipitated with an IRS-2

(Millipore # 06-506) antibody subjected to SDS page as above and then incubated with a phosphotyrosine specific antibody (Millipore #05-321).

Assessment of hearing by Auditory brainstem response (ABR)

Groups of female and male *Irs1*$^{sml/sml}$ and littermate *Irs1*$^{+/sml}$ mice (n=7–10) between 8–12 weeks of age were anesthetized with Avertin (tribromoethanol stabilized in tertiary amyl hydrate) given at a dose of 5 mg tribromoethanol/10 g body weight. Body temperature was maintained at 37–38° C by placing them on an isothermal pad in a sound-attenuating chamber. Sub-dermal needles were used as electrodes, inserted at the vertex, and ventrolaterally to each ear. Stimulus presentation, ABR acquisition, equipment control and data management were coordinated using the computerized Intelligent Hearing Systems (IHS; Miami, FL, USA). A pair of high frequency transducers were coupled with the IHS system to generate specific acoustic stimuli. Clicks, and 8, 16 and 32 kHz tone-bursts were respectively channeled through plastic tubes into the animal's ear canals. The amplified brainstem responses were averaged by a computer and displayed on the computer screen. Auditory thresholds were obtained for each stimulus by reducing the sound pressure level (SPL) at 10 dB steps and finally at 5 dB steps up and down to identify the lowest level at which an ABR pattern can be recognized (Gagnon, Longo-Guess et al. 2006).

Sample collection for phenotypic studies

For body composition and bone phenotyping (DEXA, pQCT and MicroCT) groups of female and male *Irs1*$^{sml/sml}$, littermate *Irs1*$^{+/sml}$ and *Irs1*$^{+/+}$ control mice (n=10) were necropsied and measured at 4, 8, 12 and 16 wks of age. All time points showed the same pattern and statistical significance, thus for the simplicity of presentation only the 16 wk data are reported here. For each mouse, whole body weight was recorded, whole body DEXA scans gathered, and tissue samples collected. Skeletal preparations were prepared as described previously (Beamer, Shultz et al. 2007; DeMambro, Clemmons et al. 2008). Serum was harvested from whole blood collected at necropsy and stored at −20°C until assayed for hormones.

PIXImus for areal (a)BMD

Groups of *Irs1*$^{sml/sml}$, littermate *Irs1*$^{+/sml}$ and *Irs1*$^{+/+}$ control female and male mice were measured at 4, 8, 12 and 16 wks (n = 10) for lean muscle mass, fat, and bone mineral using the PIXImus dual energy X-ray densitometer (GE-Lunar, Madison, WI, USA). The PIXImus was calibrated daily with a mouse phantom provided by the manufacturer. Mice were placed ventral side down with each limb and tail positioned away from the body. Full body scans were obtained and X-ray absorptiometry data gathered and processed with manufacturer supplied software (Lunar PIXImus 2,vers. 2.1). The head was specifically excluded from all analyses due to concentrated mineral in skull and teeth.

pQCT for volumetric (v)BMD bone densitometry

Volumetric BMD was measured on the left femur from groups (n = 10) of female and male *Irs1*$^{sml/sml}$, littermate *Irs1*$^{+/sml}$ and *Irs1*$^{+/+}$ control mice at 4, 8, 12, and 16 weeks of age. Isolated femur lengths were measured with digital calipers (Stoelting, Wood Dale, IL, USA) femurs were then measured for density using the SA Plus densitometer (Orthometrics, White Plains, NY, USA). Calibration of the SA Plus instrument was performed daily and femurs analyzed as described previously (DeMambro, Clemmons et al. 2008).

Micro-computed Tomography (MicroCT40)

Femurs from female and male *Irs1*$^{sml/sml}$, littermate *Irs1*$^{+/sml}$ and *Irs1*$^{+/+}$ control mice were scanned using MicroCT40 (Scanco Medical AG, Bassersdorf, Switzerland) to evaluate

trabecular bone volume fraction and micro-architecture in the metaphyseal region of the distal femur. In addition, cortical thickness data were obtained at the mid-shaft. The MicroCT40 unit was calibrated weekly and femurs were scanned under conditions described previously (DeMambro, Clemmons et al. 2008).

Bone Histomorphometry

To determine whether the *in vivo* histomorphometry differences seen between $Irs1^{sml/sml}$ and the $Irs1^{tm1Tka/tm1Tka}$ mice were the result of gender differences we studied groups of $Irs1^{sml/sml}$ and $Irs1^{+/+}$ females and males (n=6) at 13 weeks of age. Mice were injected with 20 mg/Kg calcein intraperitoneally (I.P.) and 50 mg/Kg demeclocycline 7 days later. Mice were sacrificed 48 hrs following the demeclocycline injection. Femurs were then analyzed as described previously (DeMambro, Clemmons et al. 2008). A separate experiment in which $Irs1^{sml/sml}$ and $Irs1^{+/sml}$ females were evaluated was then used for comparison to the $Irs1^{+/+}$ females for presence of any heterozygous effects. The terminology and units used are those recommended by the Histomorphometry Nomenclature Committee of the American Society for Bone and Mineral Research (Parfitt, Drezner et al. 1987).

Osteoblast and osteoclast cultures

Bone marrow cells were harvested from femurs and tibias of 8 wk old mice. Osteoclast-like cells were generated by plating bone marrow stromal cells at 10×10^6/well on 6 well plates in α-MEM (Invitrogen, Carlsbad, California, USA) and 10% fetal bovine serum (FBS). Osteoclast-like cells were generated by plating bone marrow stromal cells at 1×10^6 cells/well in 48 well plates in αMEM supplemented with 10 % FCS and M-CSF (30 ng/ml, PeproTech Inc, Rocky Hill, NJ, USA) and RANKL (50 ng/ml PeproTech). Cultures were maintained, fixed, stained and analyzed as described previously (DeMambro, Clemmons et al. 2008).

Mouse calvarial osteoblasts were harvested from 3–6 day old pups using standard methods (http://skeletalbiology.uchc.edu/30_ResearchProgram/304_gap/index.htm). The cells were cultured in 10% FBS α—MEM to 90% confluence and then serum starved in 0.1% FBS for 24 h to reduce cellular activity to quiescent levels. Cells were treated with insulin (100nM) or IGF-1 (100 ng/ml) for 15 min and then harvested for Western blot analysis. Data presented for cell culture experiments correspond to 3 independent experiments with at least 3 replicate cultures within each experiment.

Serum IGF-I and Insulin

Serum IGF-I levels were measured by RIA (ALPCO, Windham, NH, USA) as reported previously (Rosen, Churchill et al. 2000; Rosen, Ackert-Bicknell et al. 2004; Delahunty, Shultz et al. 2006). Serum insulin was measured by RIA (LINCO Research, St. Charles, Missouri, USA) per manufacturer's instructions. The sensitivities of the assays were 0.01 ng/ml for IGF-I and 0.1 ng/ml for insulin. The intra-assay coefficient of variation for the assays was 4.5–4.6%. All samples were analyzed within the same assay.

Glucose and Insulin Tolerance Tests

Female and male $Irs1^{sml/sml}$, $Irs1^{+/sml}$ and $Irs1^{+/+}$ mice were tested at 8 and 12 wks of age for glucose and insulin tolerance. For the glucose tolerance test, mice were placed in a clean cage with water and fasted overnight (16 hr). A 1g/Kg dose of glucose was administered I.P. and blood glucose levels were measured at 0, 20, 40, 60, and 120 min post injection. For the insulin tolerance test, mice were fed *ad libitum* and injected I.P. with insulin at a dose of 1U/Kg. Glucose levels were then measured at 0, 20, 40, 60, and 120 min post injection.

Glucose levels were measured using the OneTouch Ultra Glucometer (LifeScan, Inc., Milpitas, California, USA) per manufacturer's instructions (Messier and Kent 1995; Weitgasser, Gappmayer et al. 1999). In a separate experiment, we verified the accuracy and precision of the most recently manufactured OneTouch Ultra portable glucometers against Beckman Synchron CX5 Delta Clinical System (Beckman Coulter, Brea, CA, USA) using blood samples from 8–12 weeks old C57BL6/J mice (N=16). This comparison confirmed that glucose levels reported using portable glucometers correlated highly (r^2 =0.92) against the glucose levels reported by the Beckman Synchron CX5 Delta Clinical System (data not shown).

Statistical assessment

Statistical tests were performed using JMP version 6.0 software (SAS, Cary, NC, USA) and StatView version 5.0.1 software (SAS, Cary, NC, USA). For the DEXA, pQCT, and MicroCT40 data, differences among *Irs1*$^{sml/sml}$, *Irs1*$^{+/sml}$ and *Irs1*$^{+/+}$ mice were taken into account by including body weight and femur length as covariates in an ANCOVA model. Neither covariate was found to contribute to any of the mutant phenotypes. Data are expressed as mean ± SEM in all figures. Differences between means were tested by ANOVA, with significance declared when a $p \leq 0.05$ was observed.

Results

History of the Irs1^{sml} Mutation

The original *Irs1*^{sml} mutant was backcrossed to the C3.SW-*H2*^{b}/SnJ parental strain resulting in no mutants observed in the F1 progeny. However, the expected Mendelian ratio of 3:1 unaffected:affected for a recessive mutation was observed in the F2 progeny. Gross histological examination found no lesions in any major organs other than decreased size (data not shown). No eye defects were detected. Hearing was assessed by Auditory Brainstem Response (ABR) and both male and female mutant mice exhibited significantly higher thresholds at 8kHz, 16kHz and 32kHz than control littermates, indicative of hearing impairment in these mice (Table 2). Histological examination of the inner ear found no obvious defects.

Genetic Mapping and Mutation Analysis of the Irs1^{sml} Mutation

The F2 progeny from an intercross with CAST/Ei were used to map the *sml* mutation to Chromosome 1 between *D1Mit216* (79.8 Mb) and *D1Mit440* (90.7 Mb). Analysis of 204 F2 mice (408 meioses) positioned *sml* between *D1Mit216* (79.8 Mb, 1.23% recombination) and *D1Mit440* (90.7 Mb, 2.45% recombination). *Irs1* is located at 82.2 Mb and was considered a prime candidate for this mutation because of the smaller size of a knock out model previously reported (see introduction).

Genomic DNA from *Irs1*$^{sml/sml}$ mice and *Irs1*$^{+/+}$ controls was analyzed for the *Irs1* gene by PCR amplification using overlapping primer pairs (Table 1) and sequence analysis. We discovered a deletion of one adenine nucleotide in Exon 1 at position 1559 bp. This deletion results in a frame-shift mutation changing a glutamine to an arginine residue, which produces a premature STOP codon, predicted to result in a truncated protein of 211 amino acids instead of the full length 1233 amino acid protein.

To confirm this mutation we recognized that the deletion of the one adenine nucleotide created a restriction enzyme recognition site, which *Taq1* recognizes (T-CGA). Thus, the region of interest was amplified, and *Taq1* digestion yielded the control product of 190 bp, with a mutant product of 171 bp, confirming the deletion. Quantification of *Irs1* mRNA levels by real-time RT-PCR revealed no differences in expression between *Irs1*$^{+/+}$ and

Irs1$^{sml/sml}$ mice (data not shown). Western blot analysis of proteins from the livers of *Irs1*$^{sml/sml}$ and *Irs1*$^{+/+}$ control mice using a C-terminal specific IRS-1 antibody revealed that *Irs1*$^{sml/sml}$ mice had no detectable IRS-1 protein (Fig 1a).

Body Composition by DEXA

Homozygous male and female *Irs1*$^{sml/sml}$ mice are phenotypically recognizable at approximately 2 wks of age by their smaller size and thin short tails, a condition that persists throughout their lives despite normal GH levels. After weaning, mutants are approximately 60% the size of their *Irs1*$^{+/sml}$ control littermates, including a 20% reduction in tail length (Table 3). Whole body DEXA analysis at 16 wks of age revealed that *Irs1*$^{sml/sml}$ male and female mice had reduced % fat and aBMD compared to *Irs1*$^{+/+}$ controls. *Irs1*$^{+/sml}$ heterozygous mice had lower body weight, aBMD and % fat, than the *Irs1*$^{+/+}$ mice, but these parameters were greater than the *Irs1*$^{sml/sml}$ mutants (Table 3).

Skeletal micro-structure by pQCT and MicroCT

Analysis of femurs isolated from 16 week *Irs1*$^{+/+}$, *Irs1*$^{+/sml}$, and *Irs1*$^{sml/sml}$ mice, revealed *Irs1*$^{sml/sml}$ male and female mice had significant reductions in femur length, with an overall reduction in vBMD as measured by pQCT when compared to *Irs1*$^{+/+}$ control mice. *Irs1*$^{sml/sml}$ femurs also exhibited a reduction in cortical thickness as well as periosteal circumference (Table 3). MicroCT analysis confirmed the reduction in cortical thickness with a smaller cortical bone area/total area (% BA/TA). The distal femoral trabecular bone exhibited a significant reduction in bone volume/total volume (% BV/TV) in both the female and male *Irs1*$^{sml/sml}$ mice compared to controls (Table 3). For the female mutants, this 73% reduction in BV/TV was accompanied by a 33% decrease in trabecular number and a 42% reduction in trabecular thickness. However, the male mutants' distal femoral % BV/TV was only reduced by 29% when compared to controls. This gender difference was attributed to a 20% increase in trabecular number in the *Irs1*$^{sml/sml}$ male femurs. Although, increased in number those trabeculae were 34% thinner than controls (Table 3).

Comparison of the *Irs1*$^{+/sml}$ female and male bones to those of the *Irs1*$^{+/+}$ and *Irs1*$^{sml/sml}$ mice revealed a significant intermediate phenotype for femur length, vBMD and periosteal circumference (Table 3). Likewise a significant intermediate phenotype was found at the mid-shaft for cortical thickness and %BA/TA as measured by MicroCT. Interestingly, the heterozygous genotype did not affect % BV/TV or trabecular number in the distal femur compartment, although a slight but significant reduction in trabecular thickness was observed when compared to *Irs1*$^{+/+}$ controls (Table 3).

Histomorphometry

Histomorphometry from the distal femur of male and female *Irs1*$^{+/+}$ and *Irs1*$^{sml/sml}$ at 13 wks of age showed a marked and significant decrease in the % BV/TV analogous to what was observed by MicroCT. For both genders, the *Irs1*$^{sml/sml}$ mice had markedly reduced mineralizing surface/bone surface (%MS/BS), mineral apposition rate (MAR), and bone formation rate (BFR). Furthermore, the number of osteoblasts and osteoclasts per bone perimeter (Nob/BPm, Noc/BPm) were increased in both genders of *Irs1*$^{sml/sml}$ compared with *Irs1*$^{+/+}$ controls. However, this increase was only significant for *Irs1*$^{sml/sml}$ females (Table 4). Remarkably, there was no evidence of marrow adiposity in histological sections of the *Irs1*$^{sml/sml}$ femurs compared to the *Irs1*$^{+/+}$ femurs (Supplemental Fig 1). Inspection of the growth plate in the proximal femur revealed a marked reduction in thickness in the *Irs1*$^{sml/sml}$ mice compared to *Irs1*$^{+/+}$ consistent with their reduced bone length (Fig 2). The *Irs1*$^{+/sml}$ growth plate was also mildly reduced compared to the *Irs1*$^{+/+}$ mice.

Bone volume fraction by histomorphometry in the *Irs1*$^{+/sml}$ female mice at 13 weeks of age was not different from %BV/TV in *Irs1*$^{+/+}$ mice, akin to the findings by MicroCT. However, osteoclast numbers per bone perimeter were significantly increased ($p<0.05$) in the *Irs1*$^{+/sml}$ heterozygote mice compared to *Irs1*$^{+/+}$ females and there was a significant ($p<0.05$) reduction in mineral apposition rate (MAR) although no statistical differences were noted in overall bone formation rates nor eroded surfaces/bone surface (See Supplementary Table S1).

Cell Culture

Alkaline phosphatase (ALP) staining of bone marrow stromal cell cultures of both male and female *Irs1*$^{sml/sml}$ mice at day seven in culture revealed reductions in the number of CFU-ALP+ pre-OBs compared to *Irs1*$^{+/+}$ cultures. Similarly, at days 18 and 24 the amount of ALP staining and mineral visually detected by von Kossa staining was less in the *Irs1*$^{sml/sml}$ than *Irs1*$^{+/sml}$ heterozygotes, and both were less than the *Irs1*$^{+/+}$ control cultures (Fig 3). When non-adherent marrow cells were cultured in m-CSF and RANKL, no differences in TRAP positive multinucleated cells were seen among mutant, heterozygote or control mice (Fig 3).

To determine if the increased osteoclast number in the *Irs1*$^{sml/sml}$ mice as noted by histomorphometry was related to secretion of osteoclastogenic cytokines, we measured RANKL and OPG expression in calvarial osteoblasts and 8 week old femoral samples from *Irs1*$^{sml/sml}$ and *Irs1*$^{+/+}$ controls. There were no statistical differences in RANKL expression by real time PCR between mutants and controls from either site. Similarly for OPG, there were no strain differences noted in calvarial osteoblast expression of OPG mRNA, although in the femoral samples from *Irs1*$^{sml/sml}$ mice, there was a modest but non significant (~10%) reduction in OPG expression by real time PCR compared to controls.

Western Blot analysis of protein isolated from calvarial osteoblast cultures revealed that at *baseline*, both the *Irs1*$^{+/sml}$ and *Irs1*$^{sml/sml}$ cultures had significantly less phosphorylated AKT (pAKT) compared to *Irs1*$^{+/+}$ control cultures (Fig 1*b*). Upon stimulation with IGF-I or insulin, total AKT protein was the same across genotype, but the *Irs1*$^{+/+}$ cultures showed higher levels of AKT phosphorylation than the *Irs1*$^{sml/sml}$ and the *Irs1*$^{+/sml}$ cells. Finally, we examined the amount of IRS-2 in calvarial osteoblasts from *Irs1*$^{+/+}$, *Irs1*$^{+/sml}$ and *Irs1*$^{sml/sml}$ mice. Although total protein was the same for all three genotypes, both *Irs1*$^{sml/sml}$ and *Irs1*$^{+/sml}$ calvarial osteoblasts showed enhanced phosphorylation of IRS-2 in response to IGF-I but not insulin (Fig 4) compared to *Irs1*$^{+/+}$ osteoblasts.

Serum Analysis

Circulating levels of insulin and IGF-1 were analyzed under fasting conditions. *Irs1*$^{sml/sml}$ mice were found to be relatively hyperinsulinemic, with 3.5–4 fold higher insulin levels compared to *Irs1*$^{+/+}$ controls. Notably, heterozygous *Irs1*$^{+/sml}$ mice of both genders exhibit an intermediate phenotype marked by significantly higher serum levels of insulin compared to *Irs1*$^{+/+}$ controls but lower insulin levels compared to *Irs1*$^{sml/sml}$ mice (Fig 5a). Serum IGF-1 levels were modestly, but significantly reduced in the *Irs1*$^{sml/sml}$ mice relative to controls. In addition, a gender effect was observed in the serum IGF-I levels such that the heterozygous *Irs1*$^{+/sml}$ and *Irs1*$^{sml/sml}$ serum IGF-1 levels were significantly lower in the females than in the males of the same genotype ($p < .0005$). Unexpectedly, there was no intermediate phenotype for the *Irs1*$^{+/sml}$ males. However, in the female *Irs1*$^{+/sml}$ mice, we observed the same intermediate phenotype for serum IGF-I seen in the previous phenotypic data sets (Fig 5b).

GTT and ITT Tests

To investigate whether the mild hyperinsulinemia in *Irs1*$^{sml/sml}$ was indicative of a pre-diabetic state, glucose tolerance tests were performed on fasted *Irs1*$^{+/+}$, *Irs1*$^{+/sml}$ and *Irs1*$^{sml/sml}$ males and females at 8 wks of age (Fig 5c and 5d). At baseline, *Irs1*$^{sml/sml}$ exhibited significantly lower (30–40%) fasting glucose levels compared to controls (Fig 5c). When challenged with glucose, *Irs1*$^{sml/sml}$ glucose values rose as expected, but remained significantly lower than either *Irs1*$^{+/+}$ *or Irs1*$^{+/sml}$ levels throughout the study. Although baseline glucose levels differed, glucose levels peaked at 20 min post-injection in *Irs1*$^{sml/sml}$, as in both *Irs1*$^{+/+}$ *or Irs1*$^{+/sml}$ mice and the rate of glucose metabolism was similar among all three genotypes of mice.

For the insulin tolerance test under non-fasting conditions, the *Irs1*$^{sml/sml}$ glucose levels decreased, but not to the full extent as seen in either *Irs1*$^{+/+}$ and *Irs1*$^{+/sml}$ mice. The glucose-lowering effect of insulin, as assessed by an insulin tolerance test (Fig. 5d), revealed a mild insulin insensitivity, which was depicted as an slight, but significant, upward shift in the curve for *Irs1*$^{sml/sml}$ mice, relative to either *Irs1*$^{+/+}$ *or Irs1*$^{+/sml}$ mice (at 20, 40, 60 min intervals). By two hours post-injection of insulin, *Irs1*$^{sml/sml}$ glucose levels were comparable to those of the *Irs1*$^{+/+}$ and *Irs1*$^{+/sml}$ mice.

Discussion

In this study, we have characterized for the first time a spontaneous mutation in the *Irs1* gene that results in a pronounced metabolic and skeletal phenotype. The *Irs1*^{sml} mutation is a spontaneous frameshift mutation that results from a single nucleotide deletion in the *Irs1* gene leading to a premature stop codon and a truncated protein. This results in a hyperinsulinemic, lean, small mouse with reductions in serum IGF-I levels, BMD, and hearing. Mutant mice, although hyperinsulinemic, were only mildly insulin resistant as exogenous insulin treatment was effective in reducing circulating glucose levels. This partial ability of *Irs1*$^{sml/sml}$ mice to respond to exogenous insulin most likely prevents the development overt hyperglycemia or diabetes.

The skeletal phenotype of the *Irs1*$^{sml/sml}$ mice is remarkable and differs from genetically engineered *Irs1* null mice. *Irs1*$^{sml/sml}$ bones exhibited reductions in femur length, cortical and trabecular thicknesses and trabecular number. In addition, *Irs1*$^{sml/sml}$ mice had a pronounced reduction in mineral apposition and bone formation rates. But unexpectedly, these mutants had more osteoclasts and more osteoblasts per bone perimeter than controls. To understand the mechanism for this surprising finding we performed in vitro studies which demonstrated that *Irs1*$^{sml/sml}$ osteoblasts had impaired cell proliferation and differentiation but no differences were found in osteoclast recruitment, differentiation or appearance. Histological sections demonstrated there was adequate recruitment of osteoblast precursors; hence the defect in bone formation was likely a result of poor osteoblast function due to reduced IRS-1 signaling. Taken together we postulate that the markedly reduced bone volume fraction in the *Irs1*$^{sml/sml}$ mice is due to the inability of osteoblasts to form new bone coupled to an increase in osteoclastic activity, as evident by the larger eroded surfaces and the greater number of osteoclasts in the *Irs1*$^{sml/sml}$ mice. The absence of an in vitro effect on osteoclast differentiation from this mutation (see Fig 3b) suggests the osteoclastic changes are due to a non-cell autonomous process. In preliminary studies using real time PCR from femoral and calvarial samples, we were unable to detect differences in gene expression for RANKL, but we did find slightly lower OPG mRNA in the *Irs1*$^{sml/sml}$ bones *vs.* *Irs1*$^{+/+}$ controls. Whether the enhanced osteoblast recruitment is a compensatory response to a major defect in differentiative osteoblast function, or another process remains to be determined. But, interestingly, Zhang et al., reported that mice with a conditional *Igf1R* deletion in osteoblasts exhibited defective mineralization and had markedly increased

osteoblast numbers (Zhang, Xuan et al. 2002). This would imply there must be feedback signals that operate during terminal differentiation that attempt to compensate for impaired skeletal function.

Similarities and differences exist between this spontaneous mutation and two genetically engineered mice, *Irs1*^{tm1Tka} and *Irs1*^{tm1Jos} with knockout alleles. For example much like the *Irs1*^{sml} mutation, the *Irs1*^{tm1Tka} and *Irs1*^{tm1Jos} null mutations result in small, lean, hyperinsulinemic mice while the *Irs1*^{tm1Tka} mice have reduced areal BMD. Differences in phenotypes between the spontaneous *Irs1*$^{sml/sml}$ and the engineered *Irs1*$^{tm1Tka/tm1Tka}$ and *Irs1*$^{tm1Jos/tm1Jos}$ null mice include the lack of gender and heterozygous effects, as well as the degree of insulin resistance. Comparison of the spontaneous mutant to the *Irs1*^{tm1Tka} allele also revealed differences in osteoblast and osteoclast numbers *in vivo* vs. +/+ controls (Araki, Lipes et al. 1994; Tamemoto, Kadowaki et al. 1994; Ogata, Chikazu et al. 2000).

Phenotypic differences between the *Irs1*$^{tm1Tka/tm1Tka}$, *Irs1*$^{tm1Jos/tm1Jos}$ and the *Irs1*$^{sml/sml}$ mice may be the result of the different background strains. Reports have alluded to the importance of genetic background contributing alleles that alter bone and growth phenotypes in mutants (Gonzalez, Meyer et al. 1992; Bouxsein, Rosen et al. 2002; Martelli, Ghinassi et al. 2005). The genetically engineered *Irs1* null models are reported to be on a hybrid B6/CBA background strain whereas the *Irs1*^{sml} spontaneous mutation is on an inbred C3.SWR-*H2*^{b}/SnJ congenic strain, which contains C3H alleles at all genetic regions except for a small fixed region on Chr 17 carrying the *H2* allele. Thus, this background is more uniform compared to the segregating B6/CBA hybrid background. Modifier alleles within either background may account for the phenotypic variations observed between nulls and the spontaneous mutation.

Gender effects were not mentioned in the initial studies of the *Irs1*$^{tm1Tka/tm1Tka}$ and the *Irs1*$^{tm1Jos/tm1Jos}$ mice. Further characterization of the *Irs1*$^{tm1Tka/tm1Tka}$ mice reported no apparent differences by gender in serum IGF-I levels or in skeletal phenotyping (Ogata, Chikazu et al. 2000). However, phenotypic characterization of the *Irs1*^{sml} mutation revealed gender differences for circulating IGF-I, microarchitectural characteristics of bone, and osteoblast and osteoclast number by histomorphometry. In fact, *Irs1*$^{tm1Tka/tm1Tka}$ males are reported to have decreased numbers of both osteoblasts and osteoclasts (Hoshi, Ogata et al. 2004; Yamaguchi, Ogata et al. 2005), while the *Irs1*$^{sml/sml}$ male mice had normal numbers of both, and *Irs1*$^{sml/sml}$ female mice actually had more osteoblasts and osteoclasts. The gender effects are likely to be complex but may be a consequence of interactions involving estrogen, IGF-I signaling and bone turnover.

Ogata et al., reported no phenotypic differences between the heterozygous and +/+ controls in the *Irs1*$^{tm1Tka/tm1Tka}$ nulls (Ogata, Chikazu et al. 2000). The *Irs1*$^{+/sml}$ mice on the other hand exhibit a heterozygous phenotype for body weight, serum insulin, IGF-I, femur length, areal and volumetric BMD and body fat. Moreover, the *Irs1*$^{+/sml}$ calvarial osteoblasts have some impairment in phosphorylation of AKT that could explain the phenotypic changes. Furthermore, closer examination of bone microstructure revealed a heterozygous phenotype for the cortical compartment, such that the *Irs1*$^{+/sml}$ mice exhibit an intermediate phenotype for cortical thickness and periosteal circumference, but not in the trabecular compartment for bone volume fraction (See Table 2). On dynamic histomorphometry, the *Irs1*$^{+/sml}$ mice also had increased numbers of osteoclasts and reduced mineral apposition (MAR) compared to controls (see Table S1), suggesting that the heterozygote mouse truly exhibits an intermediate phenotype for several components of skeletal turnover. It is interesting to speculate as to why the cortical but not the trabecular component of the skeleton is affected by gene dosing. One possibility is that the increase in resorption is not as dramatic in the heterozygotes compared to the mutants, and this combined with minimal alterations in bone

formation rates result in barely detectable changes in the trabecular bone volume fraction of *Irs1*$^{+/sml}$ mice. In contrast, despite body composition change in the, the Irs1$^{+/sml}$ mice, there was no intermediate metabolic phenotype when the mice were challenged with glucose or insulin. Although no heterozygous phenotype was reported for the bones of *Irs1*$^{tm1Tka/tm1Tka}$ mice, a study done by Pete et al., did report small but significant reductions in body and organ weight in heterozygous *Irs1*$^{+/tm1Jos}$ mice (Pete, Fuller et al. 1999). Once again, it is likely that these strain differences could relate to the background of the mice and/or any compensatory effect of IRS-2 (see Fig 4) that might result from loss of a single allele in the *Irs1* gene.

Numerous studies have provided evidence of hyperinsulinemia, impaired glucose tolerance and insulin resistance in *Irs-1* null mice (Araki, Lipes et al. 1994; Tamemoto, Kadowaki et al. 1994; Yamauchi, Tobe et al. 1996; Kido, Burks et al. 2000). Initial studies on both *Irs1*$^{tm1Tka/tm1Tka}$ and *Irs1*$^{tm1Jos/tm1Jos}$ mice reported normal physiological glucose levels after fasting conditions. However, upon glucose challenge, *Irs1*$^{tm1Jos/tm1Jos}$ mice were reported to be somewhat glucose intolerant as their circulating glucose levels significantly increased compared to +/+ controls, whereas the *Irs1*$^{tm1Tka/tm1Tka}$ mice were reported to have no differences compared to +/+ controls. When *Irs1*$^{tm1Jos/tm1Jos}$ and *Irs1*$^{tm1Tka/tm1Tka}$ mice were challenged with insulin, both groups again observed significantly increased levels of glucose compared to controls, indicating insulin resistance. The *Irs1*$^{sml/sml}$ mice, on the other hand, exhibited a compensatory hyperinsulinemia due to the lack of IRS-1 but retained some insulin sensitivity, as showed by their nearly intact response to the glucose lowering effects of exogenous insulin. Further the *Irs1*$^{sml/sml}$ mice exhibited one third lower glucose levels after fasting and throughout the GTT study. This attenuated glucose response can be explained by the moderate hyperinsulinemia found in *Irs1*$^{sml/sml}$ mice.

Initial characterizations of the *Irs1*$^{tm1Tka/tm1Tka}$ mouse reported no significant differences in serum IGF-1 levels (Tamemoto, Kadowaki et al. 1994). However, Pete et al., reported a decrease in IGF-I levels in *Irs1*$^{tm1Jos/tm1Jos}$ mice compared to controls, but the change did not reach significance, most likely due to low sampling numbers (Pete, Fuller et al. 1999). In the spontaneous *Irs1*$^{sml/sml}$ mice, there is a consistent 20% decrease in IGF-I levels compared to *Irs1*$^{+/+}$ control mice. Dong et al. also reported a 20% decrease in IGF-I levels in the *Irs1*$^{tm1Jos/tm1Jos}$ mouse compared to controls (Dong, Park et al. 2006). The 20% reduction in the IGF-I serum levels in the *Irs1*$^{sml/sml}$ mice is an unexpected observation. A defect in signaling should result in increased IGF-I levels rather than a decrease, presumably as a compensatory mechanism. It is probable that, over-expression of IGF-I could partially compensate for the lack of IRS-1 in postnatal growth (Pete, Fuller et al. 1999). However, we postulate the emergence of a negative feedback loop in the absence of IRS-1 that leads to reduced IGF-I synthesis. How that inhibition occurs (perhaps locally by alterations in GH signaling) is a subject of further investigations.

We assume that the *Irs1*^{sml} mutation results in complete loss of function, but cannot rule out the possibility of a hypomorphic mutation. Indeed, it is possible that a 211 amino acid truncated peptide is produced and may bind to the IGF-I receptor by its phosphotyrosine binding (PTB) domain. If so, all the sites of binding and phosphorylation downstream of the PTB domain are missing resulting in defective signaling as evidence by the lack of AKT phosphorylation in mouse calvarial osteoblast cells when stimulated with IGF-I or insulin. This deleted region includes serine residues, which when phosphorylated, trigger protein degradation. Thus it is possible, that the truncated peptide may attach to the IGF-I receptor and perturb the system, resulting in the phenotypic differences observed between our spontaneous mutant and the engineered mutants of the *Irs1* gene. Repeated attempts to use the only commercially available N-terminus specific antibody were unsuccessful. However since the PTB domain of the IRS-1 protein is comprised of residues 144–316, our predicted

protein would contain less then 50% of the PTB domain and thus binding to the receptor is unlikely.

Reduced circulating IGF-I and mutations in the *Igf1* gene have been directly linked to hearing loss in both mice and humans (Woods, Camacho-Hübner et al. 1996; Camarero, Avendano et al. 2001; Barrenäs, Bratthall et al. 2003; Bonapace, Concolino et al. 2003; Cediel, Riquelme et al. 2006). Mice lacking the *Igf1* gene have been shown to lose many auditory neurons and exhibit increased auditory thresholds indicative of hearing impairment (Camarero, Avendano et al. 2001; Cediel, Riquelme et al. 2006). It has also been shown that IGF-I is critical in the development of the cochleovestibular ganglion in the inner ear (Varela-Nieto, Morales-Garcia et al. 2004). Furthermore, lack of IGF-I, or mutations in the *IGF-I* gene, have been associated with sensorineural hearing loss in humans (Woods, Camacho-Hübner et al. 1996; Bonapace, Concolino et al. 2003). Thus the fact that *Irs-1*^{sml} mice exhibit hearing loss further supports the existence of a major defect in the IGF-I signaling pathway.

Recently a SNP located adjacent to the *IRS-1* gene has been associated with type 2 diabetes, insulin resistance, and hyperinsulinemia in a human cohort of more than 14,000 individuals. The investigators reported a 40 % reduction in the basal levels and function of *IRS*-1 protein in the skeletal muscle of patients carrying this variant (Rung, Cauchi et al. 2009). Likewise, there are numerous studies in humans demonstrating polymorphisms in the *IRS-1* gene associated with variable responsiveness to insulin signaling (Imai, Fusco et al. 1994; Ura, Araki et al. 1996; Le Fur, Le Stunff et al. 2002). The most common polymorphism, the G972R variant, has also been associated with type II diabetes mellitus (Almind, Bjørbaek et al. 1993; Sesti 2000; Tok, Ertunc et al. 2006). However, there are no data examining the relationship between these polymorphisms and BMD or fracture risk. Based on our work combined with previous studies performed in the *Irs1* knock out models we would predict that patients with *IRS-1* polymorphisms could have a subclinical but important skeletal phenotype.

There are several limitations from our studies. First, the mechanism responsible for the low serum IGF-I levels in the *Irs1*$^{sml/sml}$ mice is not readily apparent from our data. Second, the degree of compensation between IRS-1 and IRS-2 in the mutant and heterozygote models requires further study. Third, the hyperinsulinemia along with the mild insulin resistance phenotype is intriguing and raises new questions about the importance of IRS-1 in glucose homeostasis. Fourth, the heterozygous phenotype is particularly provocative as it lends credence to the theory that similar mutations in the *IRS-1* gene may exist in humans. These are likely to be characterized by relatively modest reductions of IGF-I, low fat mass, hyperinsulinemia, reduced BMD and short stature. However, this theory will need to be verified in large population studies. Finally the increase in osteoclastogenesis in both the mutant and heterozygote mice requires further study to determine if the relatively modest reduction in OPG mRNA in the pre-osteoblasts of these mice is partly responsible for the skeletal phenotype. Notwithstanding, this paper reports the first spontaneous ‘loss of function’ mutation in the *Irs1* gene. The unique phenotypic presentation of this mutant raises new questions about the role of IRS-1 in both skeletal acquisition and glucose homeostasis.

Supplementary Material

Refer to Web version on PubMed Central for supplementary material.

Acknowledgments

The authors would like to thank Lindsay G. Horton, Colleen Kane, Belinda Harris, Leona Gagnon, Krista Delahunty, Lisa Carney, Pat Ward-Bailey and Cheryl Ackert-Bicknell for assistance with this research.

Funding

This work was supported by the National Institute of Heath (grants: **RR01183**, **ARMYLRD**, **DK042424**, **DK073267**, **AR46544** and **AR043618**).

References

Almind K, Bjørbaek C, et al. Aminoacid polymorphisms of insulin receptor substrate-1 in non-insulin-dependent diabetes mellitus. Lancet 1993;342(8875):828–832. [PubMed: 8104271]

Araki E, Lipes MA, et al. Alternative pathway of insulin signalling in mice with targeted disruption of the IRS-1 gene. Nature 1994;10(372):186–190. [PubMed: 7526222]

Atti E, Boskey AL, et al. Overexpression of IGF-binding protein 5 alters mineral and matrix properties in mouse femora: an infrared imaging study. Calcified Tissue International 2005;76(3):187–193. [PubMed: 15570402]

Barrenäs ML, Bratthall A, et al. The thrifty phenotype hypothesis and hearing problems. British Medical Journal 2003;327(7425):1199–2000. [PubMed: 14630755]

Baumann G. Mutations in the growth hormone releasing hormone receptor: a new form of dwarfism in humans. Growth Hormone & IGF Research : Official Journal of the Growth Hormone Research Society and the International IGF Research Society 1999;9 Suppl B:24–29.

Beamer WG, Shultz KL, et al. Genetic dissection of mouse distal chromosome 1 reveals three linked BMD QTLs with sex-dependent regulation of bone phenotypes. Journal of Bone and Mineral Research 2007;22(8):1187–1196. [PubMed: 17451375]

Ben Lagha N, Seurin D, et al. Insulin-like growth factor binding protein (IGFBP-1) involvement in intrauterine growth retardation: study on IGFBP-1 overexpressing transgenic mice. Endocrinology 2006;147(10):4730–4737. [PubMed: 16809446]

Bikle D, Majumdar S, et al. The skeletal structure of insulin-like growth factor I-deficient mice. Journal of Bone and Mineral Research : the Official Journal of the American Society for Bone and Mineral Research 2001;16(12):2320–2329. [PubMed: 11760848]

Bonapace G, Concolino D, et al. A novel mutation in a patient with insulin-like growth factor 1 (IGF1) deficiency. Journal of Medical Genetics 2003;40(12):913–917. [PubMed: 14684690]

Bouxsein ML, Rosen CJ, et al. Generation of a new congenic mouse strain to test the relationships among serum insulin-like growth factor I, bone mineral density, and skeletal morphology in vivo. Journal of Bone and Mineral Research 2002;17(4):570–579. [PubMed: 11918215]

Camarero G, Avendano C, et al. Delayed inner ear maturation and neuronal loss in postnatal Igf-1 deficient mice. The Journal of Neuroscience 2001;21:7630–7641. [PubMed: 11567053]

Cediel R, Riquelme R, et al. Sensorineural hearing loss in insulin-like growth factor I-null mice: a new model of human deafness. The European Journal of Neuroscience 2006;23(2):587–590. [PubMed: 16420467]

Cornish J, Callon KE, et al. Insulin increases histomorphometric indices of bone formation In vivo. Calcified Tissue International 1996;59(6):492–495. [PubMed: 8939777]

Delahunty KM, Shultz KL, et al. Congenic mice provide in vivo evidence for a genetic locus that modulates serum Insulin-like Growth Factor-1 and bone acquisition. Endocrinology 2006;147(8): 3915–3923. [PubMed: 16675518]

DeMambro VE, Clemmons DR, et al. Gender-specific changes in bone turnover and skeletal architecture in igfbp-2-null mice. Endocrinology 2008;149(5):2051–2061. [PubMed: 18276763]

Donahue LR, Beamer WG. Growth hormone deficiency in 'little' mice results in aberrant body composition, reduced insulin-like growth factor-I and insulin-like growth factor-binding protein-3 (IGFBP-3), but does not affect IGFBP-2, -1 or -4. Journal of Endocrinology 1993;136(1):91–104. [PubMed: 7679139]

Dong X, Park S, et al. Irs1 and Irs2 signaling is essential for hepatic glucose homeostasis and systemic growth. The Journal of Clinical Investigation 2006;116(1):101–114. [PubMed: 16374520]

Gagnon LH, Longo-Guess CM, et al. The chloride intracellular channel protein CLIC5 is expressed at high levels in hair cell stereocilia and is essential for normal inner ear function. The Journal of Neuroscience : the Official Journal of the Society for Neuroscience 2006;26(40):10188–10198. [PubMed: 17021174]

Garnero P, Sornay-Rendu E, et al. Low serum IGF-1 and occurrence of osteoporotic fractures in postmenopausal women. Lancet 2000;355(9207):898–899. [PubMed: 10752709]

Giustina A, Mazziotti G, et al. Growth hormone, insulin-like growth factors, and the skeleton. Endocrine reviews 2008;29(5):535–559. [PubMed: 18436706]

Godfrey P, Rahal JO, et al. GHRH receptor of little mice contains a missense mutation in the extracellular domain that disrupts receptor function. Nature Genetics 1993;4(3):227–232. [PubMed: 8395283]

Gonzalez CD, Meyer RAJ, et al. Craniometric measurements of craniofacial malformations in the X-linked hypophosphatemic (Hyp) mouse on two different genetic backgrounds: C57BL/6J and B6C3H. Teratology 1992;46(6):605–613. [PubMed: 1290161]

He J, Rosen CJ, et al. Postnatal growth and bone mass in mice with IGF-I haploinsufficiency. Bone 2006;38(6):826–835. [PubMed: 16427371]

Hoshi K, Ogata N, et al. Deficiency of insulin receptor substrate-1 impairs skeletal growth through early closure of epiphyseal cartilage. Journal of Bone and Mineral Research 2004;19(2):214–223. [PubMed: 14969391]

Imai Y, Fusco A, et al. Variant sequences of insulin receptor substrate-1 in patients with noninsulin-dependent diabetes mellitus. The Journal of Clinical Endocrinology and Metabolism 1994;79(6): 1655–1658. [PubMed: 7989470]

Janghorbani M, Feskanich D, et al. Prospective study of diabetes and risk of hip fracture: the Nurses' Health Study. Diabetes Care 2006;29(7):1573–1578. [PubMed: 16801581]

Janghorbani M, Van Dam RM, et al. Systematic review of type 1 and type 2 diabetes mellitus and risk of fracture. American Journal of Epidemiology 2007;166(5):495–505. [PubMed: 17575306]

Kido Y, Burks DJ, et al. Tissue-specific insulin resistance in mice with mutations in the insulin receptor, IRS-1, and IRS-2. The Journal of Clinical Investigation 2000;105(2):199–205. [PubMed: 10642598]

Le Fur S, Le Stunff C, et al. Increased insulin resistance in obese children who have both 972 IRS-1 and 1057 IRS-2 polymorphisms. Diabetes 2002;51 Suppl 3:S304–S307. [PubMed: 12475767]

Lienhard GE. Insulin. Life without the IRS. Nature 1994;372(6502):128–129. [PubMed: 7969441]

Liu JP, Baker J, et al. Mice carrying null mutations of the genes encoding insulin-like growth factor I (Igf-1) and type 1 IGF receptor (Igf1r). Cell 1993;75(1):59–72. [PubMed: 8402901]

Maheshwari HG, Silverman BL, et al. Phenotype and genetic analysis of a syndrome caused by an inactivating mutation in the growth hormone-releasing hormone receptor: Dwarfism of Sindh. The Journal of Clinical Endocrinology and Metabolism 1998;88(11):4065–4074. [PubMed: 9814493]

Manly KF, Cudmore RHJ, et al. Map Manager QTX, cross-platform software for genetic mapping. Mammalian Genome 2001;12(12):930–932. [PubMed: 11707780]

Martelli F, Ghinassi B, et al. Variegation of the phenotype induced by the Gata1low mutation in mice of different genetic backgrounds. Blood 2005;106(13):4102–4113. [PubMed: 16109774]

Messier C, Kent P, et al. Repeated blood glucose measures using a novel portable glucose meter. Physiology & behavior 1995;57(4):807–811. [PubMed: 7777622]

Mukherjee A, Murray RD, et al. Impact of growth hormone status on body composition and the skeleton. Hormone Research 2004;62 Suppl 3:35–41. [PubMed: 15539797]

Niu T, Rosen CJ. The insulin-like growth factor-I gene and osteoporosis: a critical appraisal. Gene 2005;361:38–56. [PubMed: 16183214]

Ogata N, Chikazu D, et al. Insulin receptor substrate-1 in osteoblast is indispensable for maintaing bone turnover. The Journal of Clinical Investigation 2000;105:935–943. [PubMed: 10749573]

Parfitt AM, Drezner MK, et al. Bone histomorphometry: Standardization of nomenclature, symbols and units. Report of the ASBMR nomenclature committee. Journal of Bone and Mineral Research 1987;2:595–610. [PubMed: 3455637]

Pete G, Fuller CR, et al. Postnatal growth responses to insulin-like growth factor I in insulin receptor substrate-1-deficient mice. Endocrinology 1999;140(12):5478–5487. [PubMed: 10579310]

Räkel A, Sheehy O, et al. Osteoporosis among patients with type 1 and type 2 diabetes. Diabetes & Metabolism 2008;34(3):193–205. [PubMed: 18308607]

Rosen C, Churchill G, et al. Mapping quantitative trait loci for serum insulin-like growth factor-1 levels in mice. Bone 2000;27:521–528. [PubMed: 11033447]

Rosen CJ, Ackert-Bicknell CL, et al. Congenic mice with low serum IGF-1 have increased body fat, reduced bone mineral density, and an altered osteoblast differentiation program. Bone 2004;35:1046–1058. [PubMed: 15542029]

Rung J, Cauchi S, et al. Genetic variant near IRS1 is associated with type 2 diabetes, insulin resistance and hyperinsulinemia. Nature genetics. 2009 **Epub ahead of print**.

Sesti G. Insulin receptor substrate polymorphisms and type 2 diabetes mellitus. Pharmacogenomics 2000;1(3):343–357. [PubMed: 11256583]

Shimoaka T, Kamekura S. Impairment of bone healing by insulin receptor substrate-1 deficiency. The Journal of Biological Chemistry 2004;279(15):15314–15322. [PubMed: 14736890]

Shirakami A, Toyonaga T, et al. Heterozygous knockout of the IRS-1 gene in mice enhances obesity-linked insulin resistance: a possible model for the development of type 2 diabetes. Journal of Endocrinology 2002;174(2):309–319. [PubMed: 12176670]

Silha JV, Mishra S, et al. Perturbations in bone formation and resorption in insulin-like growth factor binding protein-3 transgenic mice. Journal of Bone and Mineral Research 2003;18(10):1834–1841. [PubMed: 14584894]

Tamemoto H, Kadowaki T, et al. Insulin resistance and growth retardation in mice lacking insulin receptor substrate-1. Nature 1994;372(6502):182–186. [PubMed: 7969452]

Tok EC, Ertunc D, et al. Association of insulin receptor substrate-1 G972R variant with baseline characteristics of the patients with gestational diabetes mellitus. American Journal of Obstetrics and Gynecology 2006;194(3):868–872. [PubMed: 16522427]

Ura S, Araki E, et al. Molecular scanning of the insulin receptor substrate-1 (IRS-1) gene in Japanese patients with NIDDM: identification of five novel polymorphisms. Diabetologia 1996;39(5):600–608. [PubMed: 8739921]

Varela-Nieto I, Morales-Garcia JA, et al. Trophic effects of insulin-like growth factor-I (IGF-I) in the inner ear. Hearing Research 2004;196(1–2):19–25. [PubMed: 15464297]

Vestergaard P, Jørgensen JO, et al. Fracture risk is increased in patients with GH deficiency or untreated prolactinomas--a case-control study. Clinical Endocrinology 2002;56(2):159–167. [PubMed: 11874406]

Wang Y, Nishida S, et al. Role of IGF-I signaling in regulating osteoclastogenesis. Journal of Bone and Mineral Research : the Official Journal of the American Society for Bone and Mineral Research 2006;21(9):1350–1358. [PubMed: 16939393]

Weitgasser R, Gappmayer B, et al. Newer Portable Glucose Meters-Analytical Improvement Compared with Previous Generation Devices. Clinical Chemistry 1999;45:1821–1825. [PubMed: 10508129]

White MF. Insulin signaling in health and disease. Science 2003;302(5651):1710–1711. [PubMed: 14657487]

Woods KA, Camacho-Hübner C, et al. Intrauterine growth retardation and postnatal growth failure associated with deletion of the insulin-like growth factor I gene. The New England Journal of Medicine 1996;335(18):1363–1367. [PubMed: 8857020]

Yakar S, Liu JL, et al. Normal growth and development in the absence of hepatic insulin-like growth factor I. Proceedings of the National Academy of Sciences of the United States of America 1999;96(13):7324–7329. [PubMed: 10377413]

Yakar S, Rosen CJ, et al. Serum complexes of insulin-like growth factor-1 modulate skeletal integrity and carbohydrate metabolism. The FASEB Journal 2009;23(3):709–719. [PubMed: 18952711]

Yamaguchi M, Ogata N, et al. Insulin receptor substrate-1 is required for bone anabolic function of parathyroid hormone in mice. Endocrinology 2005;146:2620–2628. [PubMed: 15718274]

Yamauchi T, Tobe K, et al. Insulin signaling and insulin actions in the muscles and livers of insulin-resistant, insulin receptor substrate 1-deficient mice. Molecular and Cellular Biology 1996;116:101–114.

Zhang M, Faugere MC, et al. Paracrine overexpression of IGFBP-4 in osteoblasts of transgenic mice decreases bone turnover and causes global growth retardation. Journal of Bone and Mineral Research 2003;18(5):836–843. [PubMed: 12733722]

Zhang M, Xuan S, et al. Osteoblast-specific knockout of the insulin-like growth factor (IGF) receptor gene reveals an essential role of IGF signaling in bone matrix mineralization. The Journal of Biological Chemistry 2002;277(46):44005–44012. [PubMed: 12215457]

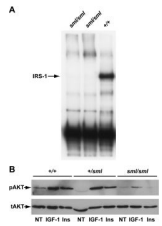

Figure 1.

Western Blots of IRS-1(A) and AKT(B). A) Liver lysates from *Irs1*$^{sml/sml}$ mice (lanes 1–2) and an *Irs1*$^{+/+}$ control (lane 3) were immunoprecipitated with an IRS-1 C-terminal specific antibody as described in methods. Following SDS-PAGE the amount of IRS-1 was determined by immunoblotting. The arrow denotes the position of the IRS-1 band which is lacking in *Irs1*$^{sml/sml}$ lysates. B) Mouse calvarial osteoblast cultures from *Irs1*$^{sml/sml}$, *Irs1*$^{+/sml}$ and *Irs1*$^{+/+}$ mice were treated with IGF-1 (IGF-1), insulin (INS) or no treatment (NT) harvested and lysed as described in the methods. Following SDS page, membranes were immunoblotted for phosphorylated AKT (pAKT) and total AKT (tAKT).

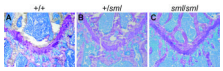

Figure 2.
Toluidine blue staining of the proximal femur growth plate at 10× magnification of 13 week old *Irs1*$^{+/+}$, *Irs1*$^{+/sml}$ and *Irs1*$^{sml/sml}$ mice.

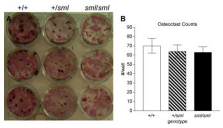

Figure 3.

Bone marrow stromal cultures (BMSC) of *Irs1*$^{sml/sml}$, *Irs1*$^{+/sml}$ and *Irs1*$^{+/+}$ control females. A) At day 18, adherent OB progenitor cells were identified by alkaline phosphatase staining (CFU-ALP) and mineralization by von Kossa staining. B) Numbers of osteoclast cells in the bone marrow stromal cultures of *Irs1*$^{sml/sml}$, *Irs1*$^{+/sml}$ and *Irs1*$^{+/+}$ mice. At day 7, the cells were fixed and stained for TRAP5b. TRAP5b positive multinucleated (>3 nuclei) osteoclasts were then counted using light microscopy. In all the experiments, male BMSC's exhibited a similar pattern as the females.

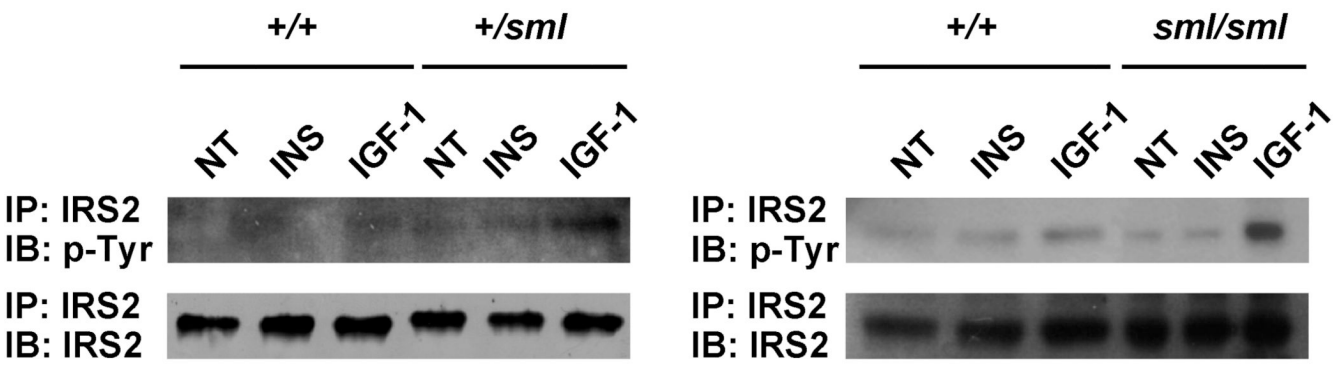

Figure 4.

Mouse calvarial osteoblast cultures from *Irs1*$^{sml/sml}$, *Irs1*$^{+/sml}$ and *Irs1*$^{+/+}$ mice were treated with IGF-1 (IGF-1), insulin (INS) or no treatment (NT) harvested and lysed as described in the methods. Lysates were immunoprecipitated with an IRS-2 antibody and then immunoblotted with IRS-2 for total protein levels or p-Tyr for phosphorylation of IRS-2.

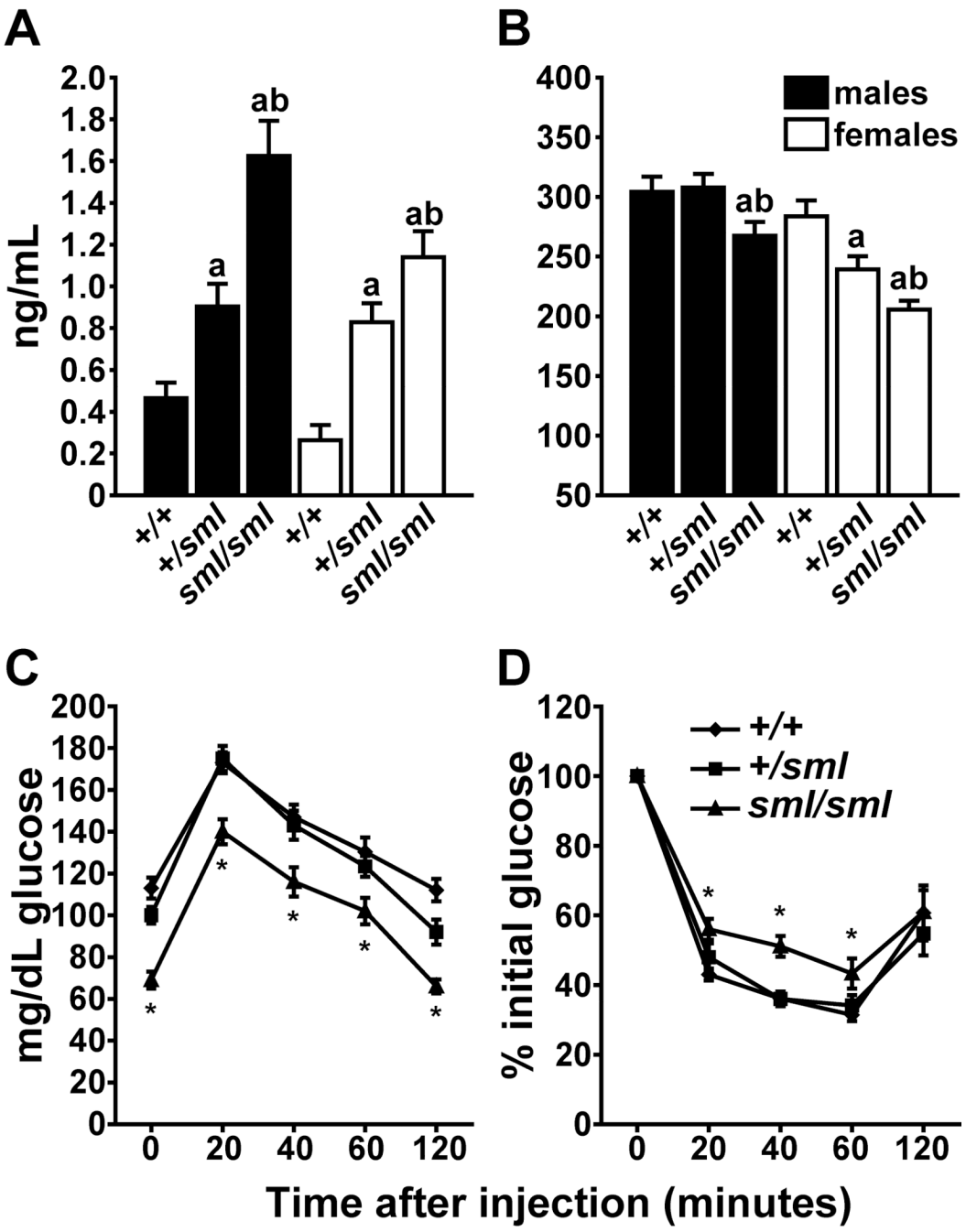

Figure 5.

Serum insulin and IGF-I levels along with glucose and insulin tolerance tests of *Irs1*$^{sml/sml}$, *Irs1*$^{+/sml}$ and *Irs1*$^{+/+}$ fasted mice. At 16 weeks of age males and females were tested for A) insulin and B) IGF-I serum levels (n=10 per genotype * = p ≤ .05 *Irs1*$^{+/sml}$ vs. *Irs1*$^{+/+}$, ** = p ≤ .05 *Irs1*$^{sml/sml}$ vs. *Irs1*$^{+/+}$ and *** = p ≤ .05 *Irs1*$^{sml/sml}$ vs. *Irs1*$^{+/sml}$). Male *Irs1*$^{+/+}$, *Irs1*$^{+/sml}$ and *Irs1*$^{sml/sml}$ at 8 weeks of age were fasted overnight and then subjected to a C) GTT or fed *ad libitum* and then subjected to a D) ITT as described in the methods. Females were tested at the same time and showed a similar pattern of significance (n=10 genotype * = p ≤ .05).

Table 1

Irs1 gene amplification and sequencing primers.

	Primer Sequence 5' to 3'	Product Size
E1-1F	GACTGGGGGAGACATAGTCC	804
E1-1R	TCCAGAGGAGCAAAACACGTGA	
E1-2F	CCTTTGCCCGATTATGCAG	794
E1-2R	TGCTCGAGTCCGATGTAGG	
E1-3F	AGTACCAGTGGCCATGGCT	856
E1-3R	CCTTTGCCCGATTATGCAG	
E1-4F	TCATTAACCCCATCAGACGC	930
E1-4R	GTGCTAGGGCTCACAGGACT	
E1-5F	CAACAGCAGCAGCAGTCTTC	818
E1-5R	AGGAGACATGGGCATATAGCC	
E1-6F	GAGCAGGGGCTGCAGTAG	826
E1-6R	CTGTTGGTCTGTGCAGCTGT	
E1-7F	GGAAGGGTCAGGGTACACAG	642
E1-7R	CTTGAGTGTCTGCGCGAAT	
E1-2F	AAAATGTAGCTTTCATTACAGCACA	583
E2-1R	AATACGGAGAGCTCACCCCT	
E2-2F	TTCATACATTGCCTCCGAGA	725
E2-2R	CTCTCCACCCAACATGAACA	
E2-3F	CCTACCTTGTGTGTTCTGGGA	433
E2-3R	CAAATTCTAAGCCGACACTTG	

Table 2

Auditory Brainstem Response in *Irs1*$^{+/sml}$ and *Irs1*$^{sml/sml}$ mice

	***+/sml* Males**	***sml/sml* Males**	***+/sml* Females**	***sml/sml* Females**
	n=7	n=9	n=10	n=12
Click	34.3 ± 1.7	51.1 ± 5.9[a]	33.5 ± 0.8	53.8 ± 5.2[a]
8 kHz	27.9 ± 4.6	50.0 ± 6.5[a]	23.5 ± 1.1	55.0 ± 6.2[a]
16 kHz	15.7 ± 4.6	34.4 ± 7.1[a]	16.0 ± 1.0	36.7 ± 5.3[a]
32 kHz	40.0 ± 2.7	61.7 ± 6.1[a]	41.0 ± 1.0	66.3 ± 5.4[a]

[a] $p<.05$ *+/sml* vs *sml/sml*

Table 3

Body composition and bone phenotype of *Irs1*$^{+/+}$, *Irs1*$^{+/sml}$, and *Irs1*$^{sml/sml}$ mice by DEXA, pQCT and MicroCT at 16 weeks of age.

	+/+ Males	**+/*sml* Males**	***sml/sml* Males**	**+/+ Females**	**+/*sml* Females**	***sml/sml* Females**
Body Weight	37.9 ± 1.0	32.3 ± 0.9^{a}	16.5 ± 0.7^{bc}	35.6 ± 1.1	31.9 ± 1.2^{a}	15.4 ± 0.4^{bc}
F. Length (mm)	15.58 ± 0.07	15.08 ± 0.11^{a}	12.55 ± 0.04^{bc}	15.47 ± 0.09	14.99 ± 0.11^{a}	12.83 ± 0.06^{bc}
% Fat	32.8 ± 0.8	28.5 ± 1.2^{a}	20.6 ± 1.9^{bc}	39.9 ± 1.4	35.3 ± 1.3^{a}	16.8 ± 1.4^{bc}
aBMD (g/cm^2)	0.057 ± 0.001	0.05 ± 0.001^{a}	0.039 ± 0.001^{bc}	0.058 ± 0.001	0.049 ± 0.001^{a}	0.038 ± 0.001^{bc}
vBMD (mm/cm^3)	0.83 ± 0.01	0.73 ± 0.01^{a}	0.65 ± 0.01^{bc}	0.86 ± 0.01	0.76 ± 0.01^{a}	0.66 ± 0.01^{bc}
Peri. Circ. (mm)	4.79 ± 0.03	4.62 ± 0.04^{a}	3.73 ± 0.02^{bc}	4.70 ± 0.02	4.28 ± 0.03^{a}	3.61 ± 0.03^{bc}
BA/TA (%)	79.0 ± 0.7	75.2 ± 1.1^{a}	71.3 ± 0.8^{bc}	81.3 ± 0.4	79.2 ± 0.6^{a}	73.9 ± 0.4^{bc}
CortTh (mm)	37.14 ± 0.66	33.26 ± 0.75^{a}	25.14 ± 0.44^{bc}	38.32 ± 0.43	34.14 ± 0.47^{a}	25.3 ± 0.20^{bc}
BV/TV (%)	22.0 ± 1.4	21.0 ± 0.8	15.4 ± 0.9^{bc}	28.3 ± 1.2	26.2 ± 0.6	7.5 ± 0.7^{bc}
TbN (mm^{-1})	4.4 ± 0.1	4.8 ± 0.1	5.3 ± 0.2^{bc}	4.2 ± 0.1	4.1 ± 0.1	2.8 ± 0.2^{bc}
TbTh (mm)	73.9 ± 2.7	66.3 ± 1.3^{a}	49.3 ± 0.7^{bc}	89.6 ± 1.1	85.5 ± 1.7^{a}	51.8 ± 0.8^{bc}

n=10

^{a}p<.05 ++ vs +/*sml*

^{b}p<.0001 +/+ vs *sml/sml*

^{c}p<.0001 +/*sml* vs *sml/sml*

F. Length, Femur Length; Peri. Circ., Periosteal Circumferance; BA/TA, Bone Area/Total Area; CortTh, Cortical thickness; BV/TV, Bone Volume/Total Volume; TbN, Trabecular Number; TbTh, Trabecular Thickness

Table 4

Histomorphometry of *Irs1*$^{+/+}$ and *Irs1*$^{sml/sml}$ distal femurs at 13 weeks of age

	+/+ Males	***sml/sml* Males**	**+/+ Females**	***sml/sml* Females**
% BV/TV	12.09 ± 0.63	7.80 ± 0.08^{a}	13.47 ± 1.63	6.94 ± 1.24^{a}
Nob/BPm (/mm)	28.00 ± 1.23	29.82 ± 2.12	27.28 ± 1.52	31.83 ± 1.05^{a}
Noc/BPm (/mm)	3.70 ± 0.37	4.32 ± 0.77	3.90 ± 0.35	5.75 ± 0.38^{a}
ES/BS (%)	12.5 ± 1.29	13.58 ± 1.69	12.87 ± 1.22	17.06 ± 0.67^{a}
MS/BS (%)	6.89 ± 0.51	2.41 ± 0.38^{a}	7.14 ± 0.84	4.10 ± 0.32^{a}
MAR (um/day)	0.441 ± 0.026	0.290 ± 0.024^{a}	0.640 ± 0.027	0.439 ± 0.047^{a}
BFR/BS (um^{3}/um^{2}/day)	0.031 ± 0.003	0.007 ± 0.001^{a}	0.046 ± 0.006	0.017 ± 0.003^{a}

n=6

* p≤.05

%BV/TV, Bone Volume/Total Volume; Tb. Th, Trabecular Thickness; Nob/BPm, number osteoblasts/bone perimeter; Noc/BPm, number osteoclasts/bone perimeter; ES/BS, eroded surface/bone surface; MS/BS, mineral surface/bone surface; MAR, mineral apposition rate; BFR/BS, bone formation rate/bone surface